2021 43rd Annual International Conference of the
IEEE Engineering in Medicine & Biology Society (EMBC)
Oct 31 - Nov 4, 2021. Virtual Conference

Euclidian-Weighted Non-linear Beamformer for Conventional Focused Beam Ultrasound Imaging Systems

Anudeep Vayyeti, *Graduate Student Member, IEEE*, and Arun K. Thittai, *Senior Member, IEEE*

***Abstract*— In this paper, the recently developed method of, Filtered Delay Euclidian-Weighted Multiply and Sum (F-D*ew*MAS), is newly investigated for Conventional Focused Beamforming (CFB) technique. The performance of F-D*ew*MAS method was compared with the established Delay and Sum (DAS) method and the popular non-linear beamforming method of F-DMAS. The different methods of F-D*ew*MAS, F-DMAS, and DAS were compared in terms of the resulting image quality metrics, Lateral Resolution (LR), Axial Resolution (AR), Contrast Ratio (CR) and contrast-to-noise ratio (CNR), in experiments on Nylon point scatterer and CIRS Triple modality Abdominal phantoms. Experimental results show that F-D*ew*MAS resulted in improvements of AR by 35.56% and 25.33%, LR by 42.97 % and 31.05 % and CR by 119.94% and 61.46% compared to those obtained using DAS and F-DMAS, respectively. The CNR of F-D*ew*MAS is 46.33 % more compared to F-DMAS. Hence, it can be concluded that the image quality is improved appreciably by F-D*ew*MAS compared to DAS and F-DMAS.**

***Keywords*— Apodization, Beamforming, Contrast Ratio, CNR, DAS, DMAS, Euclidian, F-DMAS, Hanning, Resolution, Ultrasound.**

***Clinical Relevance*—The developed method can improve the resolution and contrast of the image, which results in better visualization of finer details and thus may aid in better diagnosis.**

I. Introduction

ULTRASOUND (US) imaging is widely used for clinical applications as it is a safe and real-time modality. The beamformer is one of the most essential units of the US machine, which majorly affects the final reconstructed image quality. The primary purpose of the beamformer is to achieve a narrow main lobe with reduced side lobes since the resolution is related to the width of the main lobe, and contrast is related to the level of side lobes [1]. However, it is difficult to achieve both of them simultaneously, due to the trade-offs involved. One of the important steps during the process of beamforming is 'Apodization', where the delayed raw RF data is multiplied with weights, which reduces the side lobes with a slight increase in the width of the main-lobe, thereby, either improving or achieving desirable final reconstructed image quality [2]. In the literature, several works report the effect of different window functions (for example, Hanning, Hamming and Tukey, etc.) on the final reconstructed image quality [2-4]. Also, some works are reported on dual-apodization strategies, which tried to address the trade-offs in the main lobe and side lobe to further improve the final image quality [5, 6]. Further, adaptive and coherence-based beamformers were proposed, which change the weights for the receive aperture dynamically based on the received data statistics, or utilize spatial coherence to improve the image resolution, but with an increased computational complexity [7-11].

Recently, a non-linear beamforming method was proposed, called as Filtered Delay Multiply and Sum (F-DMAS), which utilized combinatorial processing to improve the quality of the final reconstructed image [12, 13]. In addition, several methods have been proposed to improve the F-DMAS methodology like, Double stage DMAS, Base Band DMAS (BB-DMAS), sDMAS, p-DAS [14-18]. Most recently, a weighted non-linear beamformer was proposed, namely, Filtered Delay weight Multiply and Sum (F-D*w*MAS) which utilized the advantages of both, Non-linear beamforming and apodization [19-23]. In F-D*w*MAS window coefficients raised to a certain power ('r') are multiplied to the delayed raw RF data before the process of combinatorial processing, which resulted in the improvement of resolution and contrast of the final reconstructed image for synthetic aperture based techniques [19-20]. However, F-D*w*MAS needs prior calibration for a new excitation technique, which is a disadvantage. To overcome this problem, Filtered Delay Euclidian weighted Multiply and Sum (F-D*ew*MAS) was proposed and evaluated in the context of Synthetic Aperture Technique [21]. In this paper, we are newly implementing F-D*ew*MAS beamformer for Conventional focused beamforming (CFB) to study the improvement in the final reconstructed image quality, viz-a-viz, the established Delay-and Sum and the recent non-linear beamformer of F-DMAS.

II. Materials And Methods

A. Linear (DAS) and Non-linear (F-DMAS) beamforming methods:

In DAS beamforming, in order to reconstruct a point in the medium, the raw RF data acquired over the receive aperture is delayed to make them in phase and summed, whereas, in DMAS, it is combinatorially coupled and multiplied before being summed [12]. Equation (1) and (2) give the final beamforming equations of DAS and DMAS, respectively.

$$\mathrm{DAS(t)} = \sum_{i=1}^{n} w_i(t) d_i(t) \qquad (1)$$

*Research supported by seed grant provided by IIT Madras.

Anudeep Vayyeti is with the Biomedical Engineering Group, Department of Applied Mechanics, Indian Institute of Technology Madras, Chennai, India-600036 (e-mail: am16d203@smail.iitm.ac.in).

Arun K. Thittai, is with the Biomedical Engineering Group, Department of Applied Mechanics, Indian Institute of Technology Madras, Chennai, India-600036 (corresponding author, phone: (91)-44- 2257 4053; fax: (91)-44-2257 4052; e-mail: akthittai@iitm.ac.in).

$$\mathrm{DMAS(t)} = \sum_{i=1}^{n-1} \sum_{j=i+1}^{n} d_i(t) d_j(t) \quad (2)$$

where, $d_i(t)$ and $d_i(t)$ are the delayed RF signals received by the i^{th} and j^{th} transducer elements, $w_i(t)$ is the apodization window coefficient multiplied to $d_i(t)$, and n is the number of transducer elements in receive aperture.

Further additional steps of sign preservation, dimensionality reduction and bandpass filtering were introduced in DMAS to develop filtered DMAS (F-DMAS) [12].

B. Euclidian-Weighted Non-linear (F-DewMAS) beamforming method:

In the recently proposed Filtered Delay Euclidian-weighted Multiply and Sum (F-D*ew*MAS) beamforming method, an extra stage of weighting is introduced after the delay stage. In F-D*ew*MAS, the combinatorial combinations of the window coefficients obtained after the multiplication stage are raised to the power of 'Euclidian distance' [21]. In general, these operations can be mathematically represented as in (3). The sign of the signal is preserved in (4), while (5) gives the final beamforming equation for F-D*ew*MAS.

$$x(i,j) = d(i)d(j)\big(w(i)w(j)\big)^{|i-j|} \quad (3)$$

$$y(i,j) = sign\big(x(i,j)\big).\sqrt{|x(i,j)|} \quad (4)$$

$$DewMAS(.) = \sum_{i=1}^{\frac{n^2-n}{2}} y(.) \quad (5)$$

where, $d(i)$ and $d(j)$ are the delayed RF signals received by the i^{th} and j^{th} transducer elements, respectively. $x(i,j)$ is the weighted combinatorially coupled data, $y(i,j)$ preserves the sign and finds the square root $x(i,j)$

All the other beamforming parameters, like apodization, F-number, etc., are explained in detail in reference [21]. Also, a further detailed explanation of F-D*ew*MAS beamforming method can be found in reference [21]. In this paper, Hanning was chosen as the window function without loss of generality; however, one can select any other window functions as well.

The filters applied for the various methods are listed in Table I, along with the cut-off frequencies, where the transmit frequency was 9.5 MHz.

TABLE I. FREQUENCY CUT-OFFS OF THE BP-FILTER WINDOWS FOR VARIOUS METHODS

METHOD	Pre-filter on RF signals	Post-filter after beamforming
DAS	5-14 MHz	5-14 MHz
F-DMAS	5-14 MHz	8-26 MHz
F-D*ew*MAS	5-14 MHz	8-26 MHz

The pre-filter cut-offs are chosen based on the transducer Bandwidth. Whereas, the Post-filter frequencies are selected in order to attenuate the DC and higher frequency components, while keeping the one centered at '2×center frequency' almost unaltered [12]. The post-filters were applied to the interpolated data since the sampling frequency was 40 MHz.

C. Experiments:

Experimental data were acquired with SonixTouch Q+ (Analogic Corporation, USA) Scanner using L14-5/38 transducer operating at 9.5 MHz sampled at 40 MHz. To perform the resolution study, a wire phantom was constructed and imaged. This phantom used a set of 12 wires made of Nylon having a diameter of 0.1 mm each. The wires were arranged in two columns along the depth, each column having 6 of them. This complete setup was immersed in a water bath and the cross-section of the wires was imaged. The image contrast was evaluated in experiments on commercially available 'Triple Modality 3D Abdominal Phantom (Model 057A)' (CIRS, USA)

D. Evaluation Metrics:

Axial Resolution (AR) and Lateral Resolution (LR) were estimated as the FWHM value (-6 dB) from the axial and lateral profile across the point scatterer, respectively. The Contrast Ratio (CR) and Contrast to Noise Ratio (CNR) were computed using (6) and (7), respectively, from a 3 mm x 3 mm square region of interest. CR and CNR were computed on post filtered beamformed data before log compression.

$$\mathrm{CR} = 20\log_{10}\left(\frac{\mu_t}{\mu_b}\right) \quad (6)$$

$$\mathrm{CNR} = \frac{|\mu_t - \mu_b|}{\sqrt{\sigma_t^2 + \sigma_b^2}} \quad (7)$$

where, μ_t and μ_b are the mean values of target and the background respectively, σ_t^2 and σ_b^2 are the corresponding variance.

III. RESULTS AND DISCUSSION

Fig. 1 shows the B-mode images from experiments performed on a phantom containing Nylon wire targets immersed in water. The images obtained using the different reconstruction methods of DAS, F-DMAS, and F-D*ew*MAS are compared. It can be observed that the spread of the points in the images reconstructed using F-D*ew*MAS is less compared to DAS and F-DMAS. In particular, the improvement is significant, both in lateral and axial directions, in the case of F-D*ew*MAS due to the effect of weighting methodology.

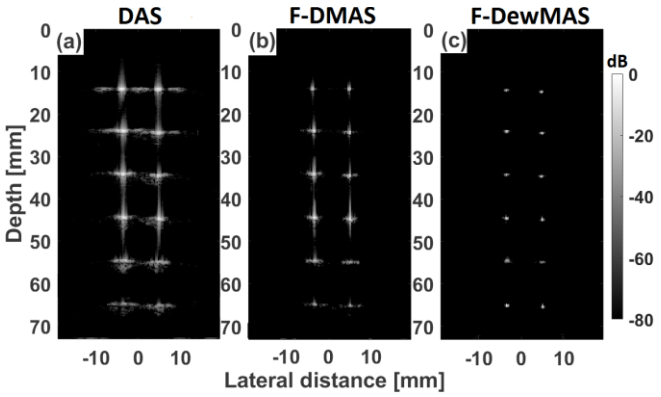

Fig. 1. B-mode images of the Nylon wire phantom immersed in water reconstructed using (a) DAS, (b) F-DMAS and (c) F-D*ew*MAS, for data acquired using CFB technique.

Fig. 2 shows the mean and standard deviations of the estimated AR and LR from the point scatterers located along the depth (for both points at that depth) for twelve independent experimental renditions, thus corresponding to 24 values. From Fig. 2 (a), it can be observed that AR of F-D*ew*MAS is better compared to DAS and F-DMAS. From Fig. 2 (b), it can also be observed that the LR of F-D*ew*MAS is also better compared to all other methods, especially, the improvement is more at greater depths. The reason for the improvement in the LR values at greater depths is due to the effect of added weighting, which reduces the contributions of the undesired signals to the spread of the point, which is indirectly related to the signal-to-noise ratio (SNR) levels. Also, Euclidian-based weights are further responsible for the reduction in the spread, which gives more weightage to the combinations that have more spatial correlation over others, thus improving the resolution.

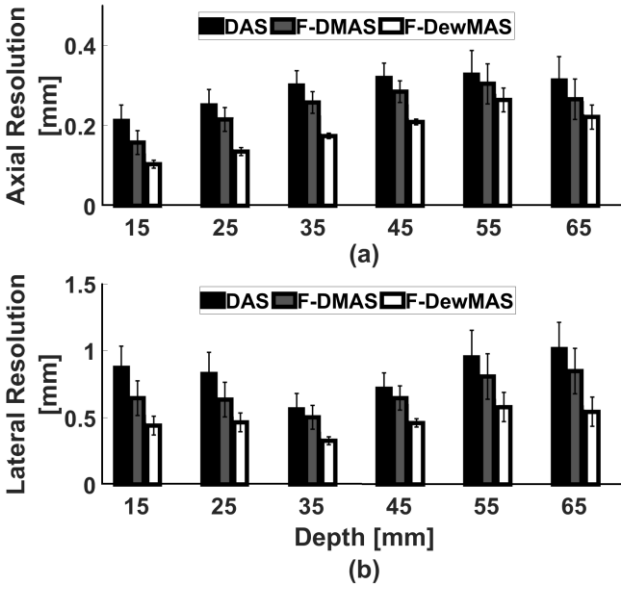

Fig. 2. Bar plots of (a) AR and (b) LR estimated from the experiments done on twelve Nylon wire targets located at different depths for various reconstruction methods.

Fig. 3 shows the B-mode images obtained from experiments on CIRS Abdominal phantom. We can observe that the cyst and the blood vessels are better contrasted with respect to background and are clearly visible with reduced noise levels in the images reconstructed with F-D*ew*MAS, as compared with those obtained using DAS and F-DMAS.

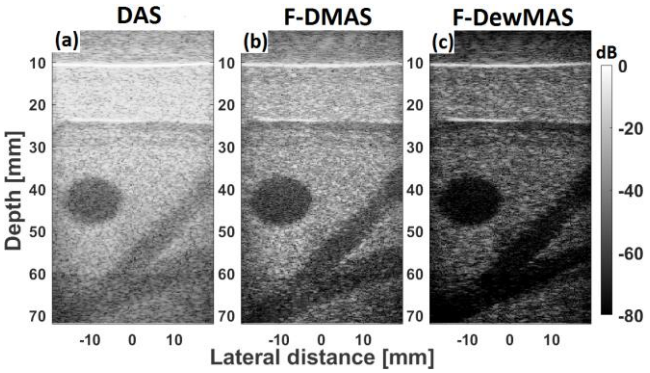

Fig. 3. B-mode images of CIRS Abdominal phantom reconstructed using (a) DAS, (b) F-DMAS and (c) F-D*ew*MAS, for data acquired using CFB technique.

Fig. 4 shows the mean and standard deviation of the estimated CR and CNR of cyst and blood vessels present along the depth from twelve independent experimental renditions. It can be observed from Fig. 4 (a) that F-D*ew*MAS have better CR compared to DAS and F-DMAS. It can be observed from Fig. 4 (b) that F-D*ew*MAS has a CNR comparable to DAS, but it is better than that from F-DMAS.

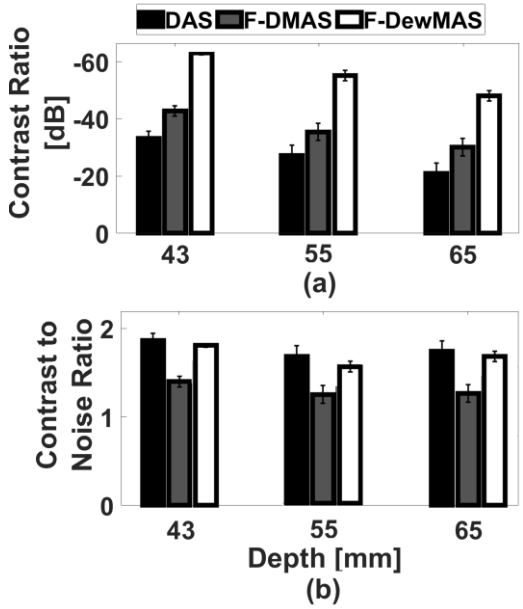

Fig. 4. Bar plots of (a) CR and (b) CNR obtained from the cyst and blood vessels located at different depths in the CIRS Abdominal phantom for various reconstruction methods is shown.

Results from experiments on phantoms show that, for the CFB technique, the F-D*ew*MAS resulted in improvements of AR by 35.56 % and 25.33%, LR by 42.97%, and 31.05 % and CR by 119.94 % and 61.46 % compared to those

obtained using DAS and F-DMAS, respectively. Also, CNR of F-D*ew*MAS is 46.33 % more compared to F-DMAS, respectively.

IV. Conclusion

Recently introduced beamformer F-D*ew*MAS is newly implemented for CFB technique. It was demonstrated that this method yields significantly improved image quality in terms of Axial Resolution, Lateral Resolution, Contrast, and Contrast to Noise Ratio compared to that obtained by either DAS or F-DMAS.

Acknowledgment

The student author, Anudeep Vayyeti, would like to thank the Ministry of Education, Government of India, for financially supporting through Half-Time Research Assistantship (HTRA) stipend. The purchase of the CIRS phantom was supported by BIRAC PACE grant #BT/AIR02648/PACE-12/17 and the Ultrasonix scanner by a Seed grant by the Institute.

References

[1] Thomenius, K.. “Evolution of ultrasound beamformers.” *1996 IEEE Ultrasonics Symposium. Proceedings* 2 (1996): 1615-1622 vol.2.W.-K. Chen, *Linear Networks and Systems* (Book style). Belmont, CA: Wadsworth, 1993, pp. 123–135.

[2] Szabo, T. L. "Diagnostic ultrasound imaging: inside out, 2nd edn, Ch. 5, 122–160." (2014).

[3] F. J. Harris, "On the use of windows for harmonic analysis with the discrete Fourier transform," in *Proceedings of the IEEE*, vol. 66, no. 1, pp. 51-83, Jan. 1978, doi: 10.1109/PROC.1978.10837.

[4] Kino, Gordon S. *Acoustic waves: devices, imaging, and analog signal processing*. Vol. 107. Englewood Cliffs, NJ: Prentice-hall, 1987.

[5] Seo, Chi Hyung, and Jesse T. Yen. "Sidelobe suppression in ultrasound imaging using dual apodization with cross-correlation." *IEEE transactions on ultrasonics, ferroelectrics, and frequency control* 55.10 (2008): 2198-2210.

[6] Chen, Yuling, and Jesse T. Yen. "Image contrast enhancement using dual apodization with cross-correlation and beamforming by spatial matched filtering." *2013 IEEE International Ultrasonics Symposium (IUS)*. IEEE, 2013.

[7] Asl, Babak Mohammadzadeh, and Ali Mahloojifar. "Minimum variance beamforming combined with adaptive coherence weighting applied to medical ultrasound imaging." *IEEE transactions on ultrasonics, ferroelectrics, and frequency control* 56.9 (2009): 1923-1931.

[8] Kim, Kyuhong, et al. "Flexible minimum variance weights estimation using principal component analysis." *2012 IEEE International Ultrasonics Symposium*. IEEE, 2012.

[9] Camacho, Jorge, Montserrat Parrilla, and Carlos Fritsch. "Phase coherence imaging." *IEEE transactions on ultrasonics, ferroelectrics, and frequency control* 56.5 (2009): 958-974.

[10] Dahl, Jeremy J., et al. "Lesion detectability in diagnostic ultrasound with short-lag spatial coherence imaging." *Ultrasonic imaging* 33.2 (2011): 119-133.

[11] Lediju, Muyinatu A., et al. "Short-lag spatial coherence of backscattered echoes: Imaging characteristics." *IEEE transactions on ultrasonics, ferroelectrics, and frequency control* 58.7 (2011): 1377-1388.

[12] Matrone, Giulia, et al. "The delay multiply and sum beamforming algorithm in ultrasound B-mode medical imaging." *IEEE transactions on medical imaging* 34.4 (2014): 940-949.

[13] Matrone, Giulia, et al. "Depth-of-field enhancement in filtered-delay multiply and sum beamformed images using synthetic aperture focusing." *Ultrasonics* 75 (2017): 216-225.

[14] Mozaffarzadeh, Moein, et al. "Double-stage delay multiply and sum beamforming algorithm applied to ultrasound medical imaging." *Ultrasound in medicine & biology* 44.3 (2018): 677-686.

[15] M. Mozaffarzadeh, A. Mahloojifar, M. Orooji, S. Adabi and M. Nasiriavanaki, "Double-Stage Delay Multiply and Sum Beamforming Algorithm: Application to Linear-Array Photoacoustic Imaging," in *IEEE Transactions on Biomedical Engineering*, vol. 65, no. 1, pp. 31-42, Jan. 2018, doi: 10.1109/TBME.2017.2690959.

[16] Shen, Che-Chou, and Pei-Ying Hsieh. "Ultrasound baseband delay-multiply-and-sum (BB-DMAS) non-linear beamforming." *Ultrasonics* 96 (2019): 165-174.

[17] Kirchner, Thomas, et al. "Signed real-time delay multiply and sum beamforming for multispectral photoacoustic imaging." *Journal of Imaging* 4.10 (2018): 121.

[18] Polichetti, Maxime, et al. "A non-linear beamformer based on p-th root compression—application to plane wave ultrasound imaging." *Applied Sciences* 8.4 (2018): 599.

[19] A. Vayyeti and A. K. Thittai, "A Filtered Delay Weight Multiply and Sum (F-DwMAS) Beamforming for Ultrasound Imaging: Preliminary Results," *2020 IEEE 17th International Symposium on Biomedical Imaging (ISBI)*, 2020, pp. 312-315, doi: 10.1109/ISBI45749.2020.9098528.

[20] A. Vayyeti and A. K. Thittai, "A Weighted Non-Linear Beamformer for Synthetic Aperture Ultrasound Imaging," *2020 IEEE International Ultrasonics Symposium (IUS)*, 2020, pp. 1-3, doi: 10.1109/IUS46767.2020.9251413.

[21] A. Vayyeti and A. K. Thittai, “Weighted non-linear beamformers for low cost 2-element receive ultrasound imaging system,” *Ultrasonics*, vol. 110, pp. 106293, Feb, 2021, doi: 10.1016/j.ultras.2020.106293.

[22] A. Vayyeti and A. K. Thittai, "A Novel Adaptively-Weighted Non-Linear Beamformer for Conventional Focused Beam Ultrasound Imaging Systems: Initial Results," *2021 IEEE International Ultrasonics Symposium (IUS)*, 2021.

[23] A. Vayyeti and A. K. Thittai, "A Novel Spatio-Temporal DMAS (ST-DMAS) Beamforming for Sparse Synthetic Aperture Ultrasound Imaging: Initial Results," *2021 IEEE International Ultrasonics Symposium (IUS)*, 2021.